Inorganic Chemistry
ARTICLE
pubs.acs.org/IC

N-Heterocyclic Carbene Ligands as Mimics of Imidazoles/Histidine for the Stabilization of Di- and Trinitrosyl Iron Complexes

Jennifer L. Hess, Chung-Hung Hsieh, Joseph H. Reibenspies, and Marcetta Y. Darensbourg*

Department of Chemistry, Texas A&M University, College Station, Texas 77843, United States

Supporting Information

ABSTRACT: N-heterocyclic carbenes (NHCs) are shown to be reasonable mimics of imidazole ligands in dinitrosyl iron complexes determined through the synthesis and characterization of a series of $\{Fe(NO)_2\}^{10}$ and $\{Fe(NO)_2\}^9$ (Enemark−Feltham notation) complexes. Monocarbene complexes (NHC-*i*Pr)(CO)Fe(NO)$_2$ (**1**) and (NHC-Me)(CO)Fe(NO)$_2$ (**2**) (NHC-*i*Pr = 1,3-diisopropylimidazol-2-ylidene and NHC-Me = 1,3-dimethylimidazol-2-ylidene) are formed from CO/L exchange with $Fe(CO)_2(NO)_2$. An additional equivalent of NHC results in the bis-carbene complexes (NHC-*i*Pr)$_2$Fe(NO)$_2$ (**3**) and (NHC-Me)$_2$Fe(NO)$_2$ (**4**), which can be oxidized to form the $\{Fe(NO)_2\}^9$ bis-carbene complexes **3**$^+$ and **4**$^+$. Treatment of complexes **1** and **2** with $[NO]BF_4$ results in the formation of uncommon trinitrosyl iron complexes, (NHC-*i*Pr)Fe(NO)$_3^+$ (**5**$^+$) and (NHC-Me)Fe(NO)$_3^+$ (**6**$^+$), respectively. Cleavage of the Roussin's Red "ester" (μ-SPh)$_2$[Fe(NO)$_2$]$_2$ with either NHC or imidazole results in the formation of (NHC-*i*Pr)(PhS)Fe(NO)$_2$ (**7**) and (Imid-*i*Pr)(PhS)Fe(NO)$_2$ (**10**) (Imid-*i*Pr = 2-isopropylimidazole). The solid-state molecular structures of complexes **1**, **2**, **3**, **4**, **5**$^+$, and **7** show that they all have pseudotetrahedral geometry. Infrared spectroscopic data suggest that NHCs are slightly better electron donors than imidazoles; electrochemical data are also consistent with what is expected for typical donor/acceptor abilities of the spectator ligands bound to the Fe(NO)$_2$ unit. Although the monoimidazole complex (Imid-*i*Pr)(CO)Fe(NO)$_2$ (**8**) was observed via IR spectroscopy, attempts to isolate this complex resulted in the formation of a tetrameric $\{Fe(NO)_2\}^9$ species, [(Imid-*i*Pr)Fe(NO)$_2$]$_4$ (**9**), a molecular square analogous to the unsubstituted imidazole reported by Li and Wang et al. Preliminary NO-transfer studies demonstrate that the $\{Fe(NO)_2\}^9$ bis-carbene complexes can serve as a source of NO to a target complex, whereas the $\{Fe(NO)_2\}^{10}$ bis-carbenes are unreactive in the presence of a NO-trapping agent.

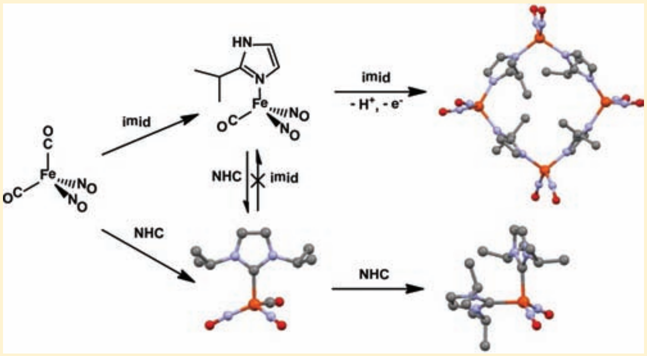

INTRODUCTION

Dinitrosyl iron complexes (DNICs) are of fundamental interest to chemists for their unique and often ambiguous redox states that have a sensitive response to spectator ligand fields. Following their discovery during animal studies some 45 years ago, it has been suggested that DNICs might function in vivo as nitric oxide storage and transfer agents.[1,2] In fact, the established degradation of iron−sulfur clusters by excess NO gives cause to question whether DNICs exist only as reporters of the deleterious effects of NO overload.[3] Regardless of their in vivo function, the readily accessible chemistry of these pseudo-organometallic units has inspired chemists to pursue the possibility that DNICs might be developed as NO-delivery pharmaceuticals.[4,5]

Throughout the past two decades, studies of DNICs have suggested that, although cysteine and glutathione are the major thiol components of cellular DNICs, N- and O-donor ligands may also trap the dinitrosyl iron moiety.[6] Only recently has a protein-bound DNIC been observed by X-ray crystallography; the Fe(NO)$_2$ unit, introduced exogenously to human glutathione transferase (GST P1-1) as bis-glutathionyl dinitrosyl iron, is found to bind within the active site of the enzyme through the phenolate oxygen of Tyr7 of the active site and the sulfur from glutathione that would normally be expected to reside in the active site.[7] While the presence of the DNIC guest, carried in with the glutathione, within this site correlates with diminished activity of GST, its identification encourages conjectures regarding protein chaperones or transport agents.

To date, most potential models of biological DNICs have relied on thiolate ligands that give rise to monomeric $[(RS)_2Fe(NO)_2]^-$ as well as dimeric, Roussin's red-ester type complex forms, that is, (μ-RS)$_2$[Fe(NO)$_2$]$_2$.[8−12] In both, the Fe(NO)$_2$ is in its oxidized form of $\{Fe(NO)_2\}^9$ electron configuration according to Enemark−Feltham notation.[13] Phosphine DNICs are known (stabilizing the reduced $\{Fe(NO)_2\}^{10}$ redox level) as well as DNICS containing nitrogen donors, particularly those mimicking the coordination of the histidine amino acid residue, frequently found as an adjunct to cysteine in metallobiomolecules.[14−16] A recent study by Tinberg and Lippard et al. looked for evidence of both (Cys-S)$_2$Fe(NO)$_2^-$ and

Received: May 27, 2011
Published: August 08, 2011

dx.doi.org/10.1021/ic201138f | *Inorg. Chem.* 2011, 50, 8541–8552

$(His\text{-}N)_2Fe(NO)_2$ that might be derived from a Rieske-type ferredoxin protein.[17] Excess NO (or a NO-donor molecule) was reacted with the toluene/*o*-xylene monooxygenase component C (ToMOC) from *Pseudomonas* sp. OX1), containing a [2Fe-2S] cluster with two histidines and two cysteine ligands on individual irons. The observation of an EPR signal characteristic of a $\{Fe(NO)_2\}^9$ unit supported the expectation of bis-cysteine DNIC as seen with common 4Fe-4S clusters,[18] or of one of the possible forms of bis-histidine within an oxidized DNIC. As EPR spectroscopy is the major tool for detecting DNICs, the authors stated that the formation of the histidine-bound $\{Fe(NO)_2\}^{10}$ product was not verified but cannot be ruled out.[17]

In contrast to cysteine, histidine binding to metals offers additional complexities, including the basic nitrogen as a neutral donor and, on deprotonation of the weakly acidic N−H, a 1^- donor is obtained. Consequently, there are three possibilities for $(His)_2Fe(NO)_2$ complexes: a neutral EPR inactive $\{Fe(NO)_2\}^{10}$ complex, a neutral EPR active $\{Fe(NO)_2\}^9$ complex, or an anionic EPR active $\{Fe(NO)_2\}^9$ complex. It is expected that the bioactivity of histidine-containing DNICs could critically depend on differences derived from these various redox/protonation levels.

Li and co-workers have approached the difficult task of modeling histidine-containing DNICs and have ν(NO) infrared values for several neutral $(imidazole)_2Fe(NO)_2$ complexes mostly characterized in situ.[19] In one case, a neutral $(Imid\text{-}Me)_2Fe(NO)_2$ (Imid-Me = 1-methylimidazole) complex of $\{Fe(NO)_2\}^{10}$ electron configuration was isolated and structurally characterized (Figure 1a).[14] The extreme air sensitivity of this complex and all other members of the series led to detection of the oxidized $\{Fe(NO)_2\}^9$ species by EPR spectroscopy, presumably arising from adventitious O_2 as an oxidant.[14,19] As in the $(RS)_2Fe(NO)_2^-$ complexes, the characteristic EPR signal is ∼2.03.[8−12]

The N-heterocyclic carbene (NHC) ligands have gained widespread use in organometallic chemistry for their strong σ-donating characteristics and ability to bind to and stabilize a range of transition-metal complexes.[21,22] An example appropriate to Fe-NO chemistry is the observation of a trinitrosyl iron complex (TNIC) ligated by 1,3-bis(2,4,6-trimethylphenyl)imidazol-2-ylidene (NHC-Mes, Figure 1c) that can be readily isolated and manipulated in solution under ambient conditions; the analogous $(R_3P)Fe(NO)_3^+$ (R = *p*-tolyl) immediately decomposes in solution at room temperature (22 °C).[20]

The planar NHC ligands mimic ligands, such as imidazoles and pyridine; steric and electronic properties of the NHCs are largely influenced by the substituents on the N atoms of the NHC ring. A structural comparison of three imidazoles with the dimethyl NHC complexed to square-planar $Ni(N_2S)$, Ni(mmp-dach) (mmp-dach = 1-(2-mercapto-2-methyl-propyl-1,4-diazacycloheptane), found in all cases the plane of the ligands to be perpendicular to the NiN_2S plane with no significant differences in the $Ni{-}N_{Imid}$ and $Ni{-}C_{NHC}$ distances (1.89−1.90 Å), as well as the Ni−N or Ni−S spectator ligand distances (Figure 2).[23] The barrier to rotation about the Ni−N bond of the imidazoles was experimentally determined by VT ^1H NMR studies, finding that, for nonsterically hindered methylimidazole, $\Delta G^{\ddagger}$ = 8.97 kcal/mol, a value that was corroborated by DFT calculations. In contrast, the NHC derivative was sterically prohibited from such intramolecular dynamics over the accessible temperature range.[23]

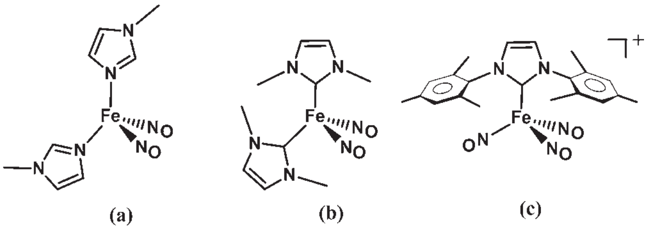

Figure 1. Model complexes of histidine-containing $\{Fe(NO)_2\}^{10}$ DNIC: (a) $(Imid\text{-}Me)_2Fe(NO)_2$ (Imid-Me = 1-methylimidazole),[14] (b) $(NHC\text{-}Me)_2Fe(NO)_2$ (NHC-Me = dimethyl N-heterocyclic carbene), and (c) $(NHC\text{-}Mes)Fe(NO)_3^+$ (NHC-Mes = 1,3-bis(2,4,6-trimethylphenyl) N-heterocyclic carbene).[20]

Crabtree and Eisenstein have described DFT computational results relating to the possibility of tautomerization from the N-bound to C-bound form of histidine in several metal derivatives of imidazoles (eq 1). They concluded that N-binding is more favorable for first-row elements, whereas C-binding is preferred by second- and third-row elements. Additionally, C- versus N-binding could be influenced by an imposed hydrogen-bonding network around the histidine.[24] It should also be noted that the general preparation of NHCs involves the facile alkylation of imidazoles (eq 2).[25] Furthermore, histidinium salts have been known to react with Ag^I, Pd^{II}, or Rh^I sources to form the respective transition-metal NHC complex.[26] Such interconversions between imidazole and NHC are intriguing possibilities for biological systems, as yet undiscovered.

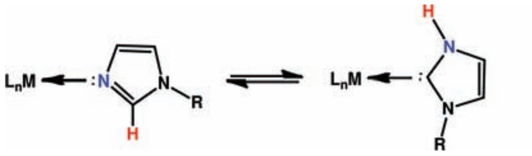

(1)

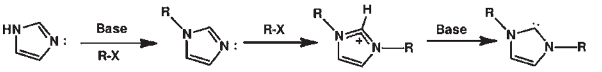

(2)

To further explore the analogy described above, as well as to develop the synthetic chemistry relating to $Fe(NO)_2$ as NO releasing agents, we present a series herein of DNICs containing NHCs and imidazoles in both the reduced $\{Fe(NO)_2\}^{10}$ and the oxidized $\{Fe(NO)_2\}^9$ forms as mimics of histidine-containing DNICs.

■ EXPERIMENTAL SECTION

General Methods and Materials. All solvents were reagent grade and were purified and degassed by a Bruker solvent purification system and stored over molecular sieves. Reagents, including nitrosonium tetrafluoroborate, 1,3-diisopropylimidazolium tetrafluoroborate, sodium *tert*-butoxide, sodium thiophenolate, 2-isopropylimidazole, and 5,10,15,20-tetraphenyl-21*H*,23*H*-porphine cobalt(II), Co(TPP), were purchased from Sigma-Aldrich Chemical Co. and were used as received. Standard Schlenk-line techniques (N_2 atmosphere) and an Ar-filled glovebox were used to maintain anaerobic conditions during preparation, isolation, and product storage. $Fe(CO)_2(NO)_2$,[27] [Na-18-crown-6-ether][$Fe(CO)_3(NO)$],[28] and 1,3-dimethylimidazolium iodide[25] were prepared according to published procedures.

Physical Measurements. Infrared spectra were recorded on a Bruker Tensor 27 FTIR spectrometer in CaF_2 solution cells with a path length of 0.1 mm. Mass spectrometry (ESI-MS) was performed by the Laboratory for Biological Mass Spectrometry at Texas A&M University.

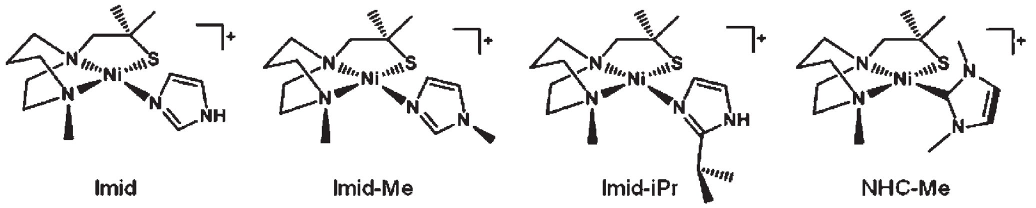

Figure 2. Structures of $[LNi(N_2S)]^+$ complexes where the plane of L is perpendicular to the NiN_2S plane. L = Imid (imidazole), Imid-Me (1-methylimidazole), Imid-*i*Pr (2-isopropylimidazole), and NHC-Me (dimethyl N-heterocyclic carbene).[23]

Nanoelectrospray ionization in positive mode was performed using an Applied Biosystems QSTAR Pulsar (Concord, ON, Canada) equipped with a nanoelectrospray ion source. Solution was flowed at 700 nL/min through a 50 μm ID fused-silica capillary that was tapered at the tip. Electrospray needle voltage was held at 1900 V.

Elemental analyses of crystalline samples were determined by Atlantic Microlab, Inc., Norcross, GA. The poor match of found to calculated values of several samples is likely due to their sensitivity and resulting instability when exposed to O_2. EPR spectra were typically recorded in frozen THF using a Bruker ESP 300 equipped with an Oxford ER910 cryostat operating at 10 K. The WinEPR Simfonia program was used to simulate spectral parameters.[29] Cyclic voltammograms were recorded on a BAS-100A electrochemical analyzer. All experiments were performed at room temperature under an Ar blanket in THF solution containing 0.1 M $[t\text{-}Bu_4N][BF_4]$ as the electrolyte, with a 3.0 mm glassy carbon working electrode, a $Ag/AgNO_3$ reference electrode, and a Pt coil counter electrode. All values have been internally referenced to Cp_2Fe/Cp_2Fe^+. The mass magnetic susceptibility, χ_g, of a crystalline sample of complex **9** was measured (Gouy balance at 299 K) as 0.057×10^{-4} erg·G^{-2} cm^{-3}.

X-ray Crystallography. Crystal samples were coated in mineral oil, affixed to a Nylon loop, and placed under streaming N_2 (110 K) in a Bruker SMART 1000 CCD or single-crystal APEXii CCD diffractometer. X-ray diffraction data were collected by covering a hemisphere of space upon combination of three sets of exposures. The structures were solved by direct methods. H atoms were placed at idealized positions and refined with fixed isotropic displacement parameters, and anisotropic displacement parameters were employed for all non-hydrogen atoms. The following programs were used: for data collection and cell refinement: SMART WNT/2000, version 5.632[30] or APEX2;[31] data reductions, SAINTPLUS, version 6.63;[32] absorption correction, SADABS;[33] structure solutions, SHELXS-97;[34] and structure refinement, SHELXL-97.[35] Structure plots were generated in Mercury, version 2.3.[36]

Preparation of Compounds. *(NHC-iPr)(CO)Fe(NO)$_2$, Complex* ***1***. In a 100 mL Schlenk flask, 1.00 g (2.20 mmol) of [Na-18-crown-6-ether]$[Fe(CO)_3(NO)]$ and 0.26 g (2.23 mmol) of $[NO]BF_4$ were dissolved in 15 mL of THF and stirred for at least 10 min to produce $Fe(CO)_2(NO)_2$, which was vacuum-transferred to a flask immersed in liquid N_2. A separate flask loaded with 0.52 g (2.18 mmol) of 1,3-diisopropylimidazolium tetrafluoroborate and 0.21 g (2.21 mmol) of NaO^tBu was dissolved in 5 mL of THF and stirred for at least 30 min. This pale yellow solution was transferred via a cannula to the flask of $Fe(CO)_2(NO)_2$ in THF, and the mixture was stirred for at least an hour, resulting in a brown opaque mixture. The solvent was removed in vacuo, and a minimum amount of THF was added (~2 mL), followed by 30−40 mL of hexanes. This mixture was filtered through Celite, and the filtrate was dried in vacuo and then dissolved in a minimum amount of pentane. The pentane solution was transferred via a "football" cannula (5.5 cm filter paper folded around and affixed to one end of the cannula with Teflon tape) to several stoppered and degassed test tubes, which were stored at 0 °C. Within several days, X-ray quality red-brown crystals were obtained. Isolation of the crystals afforded 0.24 g (37% yield) of product. $FeC_{10}H_{16}N_4O_3$ (MW = 296 g/mol) $^+$ESI-MS: m/z = 309 $[M - CO + CH_3CN]$; 268 $[M - CO]$; 238 $[M - CO - NO]$. IR (THF): ν(CO) 1986 (m), ν(NO) 1738 (m), 1696(s) cm^{-1}. Anal. Calcd (found): C, 38.2 (38.7); H, 5.74 (6.31); N, 17.8 (15.1).

(NHC-Me)(CO)Fe(NO)$_2$, Complex ***2***. In a similar manner to that described above, $Fe(CO)_2(NO)_2$ was freshly prepared and added to a mixture of 0.49 g (2.19 mol) of 1,3-dimethylimidazolium iodide and 0.21 g (2.19 mmol) of NaO^tBu in 5 mL of THF to ultimately produce 0.23 g (44.3%) of a red-brown crystalline solid. X-ray quality crystals were obtained by evaporation of pentane from the product mixture at 0 °C. $FeC_6H_8N_4O_3$ (MW = 240 g/mol) $^+$ESI-MS: m/z = 287 $[M - CO + CH_3CN]$ IR (THF): ν(CO) 1988 (m), ν(NO) 1740 (m), 1697 (s) cm^{-1}. Anal. Calcd (found): C, 30.0 (29.6); H, 3.34 (3.71); N, 23.4 (21.6).

(NHC-iPr)$_2$Fe(NO)$_2$, Complex ***3***. A pale yellow solution of NHC-*i*Pr (prepared from 0.19 g (0.81 mmol) of 1,3-diisopropylimidazolium tetrafluoroborate and 0.078 g (0.81 mmol) in 5 mL of THF) was transferred via a cannula to a flask charged with 0.24 g (0.80 mmol) of complex **1** in 10 mL of THF. The reaction mixture was stirred overnight and then dried in vacuo. A 40 mL portion of hexanes was added, the mixture was stirred for 10 min, and the supernatant was separated from the precipitate via a "football" cannula. The precipitate was dissolved in THF and filtered through Celite. The solution was concentrated in vacuo, transferred to several degassed test tubes, and layered with hexanes to produce X-ray quality green-brown crystals at 0 °C. Isolation of the crystals afforded 0.13 g (38.0%) of analytically pure product. $FeC_{18}H_{32}N_6O_2$ (MW = 419 g/mol) $^+$ESI-MS: m/z = 420 $[M + H]^+$. IR (THF): ν(NO) 1664 (m), 1619 (s) cm^{-1}. Anal. Calcd (found): C, 49.3 (49.3); H, 7.77 (7.62); N, 19.2 (18.5).

(NHC-Me)$_2$Fe(NO)$_2$, Complex ***4***. In a similar manner to that described above, a mixture of 0.14 g (0.60 mmol) of 1,3-dimethylimidazolium iodide and 0.058 g (0.60 mmol) of NaO^tBu dissolved in 5 mL of THF was added to a flask charged with 0.14 g (0.60 mmol) of complex **2** in 10 mL of THF, ultimately producing 0.034 g (18.3%) of a brown crystalline solid. A THF solution of **4** was layered with hexanes at 0 °C to obtain X-ray quality crystals. $^+$ESI-MS of $FeC_{10}H_{16}N_6O_2$ (FW = 307 g/mol): m/z = 308 $[M + H]^+$, 278 $[M - NO]$. IR (THF): ν(NO) 1667 (m), 1624 (s) cm^{-1}. Anal. Calcd for $FeC_{10}H_{16}N_6O_2$ (found): C, 39.0 (37.6); H, 5.23 (5.12); N, 27.3 (25.5).

[(NHC-iPr)Fe(NO)$_3$][BF$_4$], Complex ***5***$^+$. A 0.056 g (0.19 mmol) sample of complex **1** was dissolved in 10 mL of THF and transferred via a cannula to a Schlenk flask containing 0.024 g (0.21 mmol) of $[NO]BF_4$. The mixture was stirred for 1 h, resulting in a green precipitate, which was filtered and washed with THF and ether to afford 0.026 g (35.7%) of a green powder. X-ray quality crystals were obtained by layering a CH_2Cl_2 solution of the product with hexanes at 0 °C. IR (CH_2Cl_2): ν(NO) 1915 (m), 1826 (sh), 1810 (s) cm^{-1}. Anal. Calcd for $C_9H_{17}B_1F_4Fe_1N_5O_3$ (found): C, 28.1 (28.6); H, 4.19 (4.12); N, 18.2 (17.8).

[(NHC-Me)Fe(NO)$_3$][BF$_4$], Complex ***6***$^+$. In a similar manner to that described above, 0.097 g (0.34 mmol) of complex **2** was dissolved in 10 mL of THF and transferred via a cannula to a flask containing 0.037 g (0.32 mmol) of $[NO]BF_4$. Isolation of the precipitate afforded 0.050 g (48.1%) of a green solid. IR (CH_2Cl_2): ν(NO) 1915 (m), 1826 (sh), 1814 (s) cm^{-1}. The green powder was not stable, even under an

anaerobic environment, resulting in decomposition to an insoluble tan solid and loss of ν(NO) IR bands.

[(NHC-iPr)$_2$Fe(NO)$_2$][BF$_4$], Complex $\mathbf{3^+}$. A 0.024 g (0.10 mmol) sample of 1,3-diisopropylimidazolium tetrafluoroborate and 0.010 g (0.10 mmol) of Na^{t}OBu were dissolved in 10 mL of CH_2Cl_2 and stirred for at least 30 min prior to transfer to a Schlenk flask containing 0.044 g (0.11 mmol) of complex $\mathbf{5}^+$ in 5 mL of CH_2Cl_2. The solution was stirred for 30 min, and then the solvent was reduced in vacuo. About 20−30 mL of hexanes was added to the mixture to precipitate out a brown powder (0.015 g, 29.6%). $^+$ESI-MS for $FeC_{18}H_{32}N_6O_2(BF_4)$ (MW = 420 g/mol): m/z = 420 [M]$^+$; 390 [M − NO]. IR (THF): ν(NO) 1789 (m), 1733 (s) cm^{-1}. The powder slowly degrades over the course of several days at 22°, even under an anaerobic environment, resulting in decomposition to an insoluble orange-brown solid and loss of ν(NO) IR bands. In solution under N_2, complex $\mathbf{3}^+$ as the BF_4^- (as well as the PF_6^-) salt is largely stable over the course of 8 h; however, within 24 h, there is major decomposition.

[(NHC-Me)$_2$Fe(NO)$_2$][BF$_4$], Complex $\mathbf{4^+}$. In a manner similar to that above, 0.014 g (0.063 mmol) of 1,3-dimethylimidazolium iodide and 0.006 g (0.062 mmol) of Na^{t}OBu were dissolved in 5 mL of CH_2Cl_2 and stirred for 30 min. This mixture was transferred to a Schlenk flask containing 0.020 g (0.061 mmol) of complex $\mathbf{6}^+$ in 5 mL of CH_2Cl_2 to yield a yellow-brown solution. The unstable product was detected in solution by IR (THF): ν(NO) 1791 (m), 1723 (s) cm^{-1} and mass spectrometry $FeC_{10}H_{16}N_6O_2(BF_4)$ (MW = 308 g/mol) $^+$ESI-MS: m/z = 308 [M]$^+$. Over the course of an hour, the color of the solution bleaches, ν(NO) IR bands disappear, and an insoluble orange-brown precipitate forms.

(NHC-iPr)(PhS)Fe(NO)$_2$, Complex ***7***. *Method A.* A 0.027 g (0.11 mmol) sample of 1,3-diisopropylimidazolium tetrafluoroborate and 0.011 (0.11 mmol) g of NaO^{t}Bu were dissolved in 10 mL of THF and stirred for 30 min prior to transfer to a Schlenk flask containing 0.025 g (0.056 mmol) of the Roussin's Red ester (μ-SPh)$_2$[Fe(NO)$_2$]$_2$[38] in 5 mL of THF. The solution was stirred for 30 min, and then the solvent was removed in vacuo. The resulting dark purple-red residue was dissolved in a minimum amount of pentane (∼10 mL) and portioned out to three degassed and stoppered test tubes. This process was repeated several times until the entire product was dissolved in pentane and transferred to test tubes. The test tubes were put in the freezer at 0 °C overnight to afford 0.030 g (71.4%) of dark red crystalline material. X-ray quality crystals were obtained via slow evaporation from ether solution at 0 °C. $FeC_{15}H_{21}N_4O_2S$ (MW = 377 g/mol) $^+$ESI-MS: m/z = 378 [M + H]$^+$. IR (THF): ν(NO) 1757 (m), 1712 (s) cm^{-1}. Anal. Calcd for $FeC_{15}H_{21}N_4O_2S$ (found): C, 47.8 (47.9); H, 5.57 (5.68); N, 14.9 (14.7).

Method B. A 0.036 g (0.094 mmol) sample of complex $\mathbf{5}^+$ was dissolved in 10 mL of CH_2Cl_2 and transferred to a Schlenk flask loaded with excess NaSPh (0.022 g, 0.17 mmol). The mixture was stirred for 30 min, resulting in a red solution. The solvent was removed in vacuo, and the residue was extracted with 20 mL of CH_2Cl_2 and filtered through Celite. Removal of solvent resulted in 0.021 g (74.7%) of a dark red solid. Product from this route and that of method A above had identical properties. Method A is, however, preferred for simplicity.

(Imid-iPr)(CO)Fe(NO)$_2$, Complex ***8***. Fresh $Fe(CO)_2(NO)_2$ in 10 mL of THF was prepared following the procedure described above for the preparation of complex **1** using 0.50 g (1.10 mmol) of [Na-18-crown-6-ether][$Fe(CO)_3(NO)$] and 0.13 g (1.11 mmol) of [NO]BF_4. A 0.12 g (1.1 mmol) sample of 2-isopropylimidazole (Imid-*i*Pr) in 10 mL of THF was added via a cannula and stirred for 1 h. The IR spectrum (ν(CO) THF solution: 1992 (s); ν(NO) 1744 (m), 1698 (s) cm^{-1}) indicated formation of expected product; however, conversion to a tetramer (see the following for complex **9**) occurred upon attempts to isolate product.

[(Imid-iPr)Fe(NO)$_2$]$_4$, Complex ***9***. Attempts to form and isolate (Imid-*i*Pr)$_2$Fe(NO)$_2$ with addition of 1 equiv of Imid-*i*Pr to complex **8** were unsuccessful and led to the isolation of a tetramer. The optimized procedure for complex **9** is as follows: Fresh $Fe(CO)_2(NO)_2$ in CH_2Cl_2 was prepared following the procedure above using 0.75 g (1.64 mmol) of [Na-18-crown-6-ether][$Fe(CO)_3(NO)$] and 0.20 g (1.71 mmol) of [NO]BF_4. A 0.36 g (3.3 mmol) portion of Imid-*i*Pr in 15 mL of CH_2Cl_2 was added via a cannula, and the mixture was stirred overnight. [Note: Shorter reaction times could be achieved on deliberate addition of oxygen to the reaction vessel; however, excess oxygen degrades the product. Hence, best results were obtained as described above with adventitious oxygen presumably serving as an oxidant.] The solvent was removed in vacuo from the green-brown solution, and 30−40 mL of hexanes was added and filtered through Celite. The solvent was removed in vacuo to afford 0.072 g (19.5%) of the red-brown solid product. X-ray quality crystals were grown via evaporative removal of solvent from an ether solution at 0 °C. IR (THF): ν(NO) 1794 (m), 1726 (s) cm^{-1}. EPR: broad rhombic signal at 2.03. Mass spectrometry (Nano-(+)-ESI MS): low intensity parent ion ($Fe_4N_{16}O_8C_{24}H_{36}$) isotope bundle centered at m/z = 900, base (100%) peak centered at 538 ($Fe_3N_9O_5C_{12}H_{18}$, representing $Fe_3(NO)_5$(Imid-*i*Pr)$_2$), other intense bundles centered at m/z 478.8 represent loss of 2NO from the base peak and at 647.9 representing addition of one Imid-*i*Pr (+110 mass units) to the base peak. The full mass spectrum is in the Supporting Information. Complex **9** reacted with [Na-18-crown-6-ether]$^+$ imidazolate-*i*Pr$^-$ (formed by deprotonation of Imid-*i*Pr in THF solvent by Na^0 in the presence of 18-crown-6-ether) to yield a compound of IR and EPR parameters (see Tables 3 and 5) similar to that of [Na-18-crown-6-ether][(Imid)$_2$Fe(NO)$_2$].[15]

NO-Trapping Experiments. Yellow-brown complex $\mathbf{3}^+$ was formed in situ according to the procedure described above and transferred via a cannula to a Schlenk flask containing Co(TPP) (0.013 g, 0.019 mmol in 10 mL of THF, Co(TPP) = 5,10,15,20-tetraphenyl-21*H*,23*H*-porphine cobalt(II)). Within minutes, an absorption band at 1683 cm^{-1} assignable to (NO)Co(TPP) appeared and continued to grow in over the course of 6 h, along with a distinct color change of the solution from dark brown-red to red. The reaction mixture was monitored by IR spectroscopy for 24 h. A decrease of complex $\mathbf{3}^+$ IR bands at 1789 and 1733 cm^{-1} and an increase of the band at 1683 cm^{-1} were taken as an indication of NO transfer.[37] The same procedure was performed for complex **3** (0.010 g, 0.024 mmol) with Co(TPP) (0.016 g 0.024 mmol); however, the IR bands associated with complex **3** did not decrease and the band at 1683 cm^{-1} characteristic of (NO)Co(TPP) was not observed.

■ RESULTS AND DISCUSSION

Synthesis, Isolation, and Physical Properties. Synthetic access to reduced $\{Fe(NO)_2\}^{10}$ DNICs relies on the freshly prepared $Fe(CO)_2(NO)_2$ precursor, with CO/L exchange readily occurring for both L = N-heterocyclic carbenes (NHC) and imidazoles. As noted in Scheme 1, on addition of 1 equiv of NHC, the mono-NHC complexes **1** and **2** were obtained, and with 2 equiv of NHC, disubstituted complexes **3** and **4** were formed. Complex **8** was observed with reaction of the $Fe(CO)_2(NO)_2$ precursor with 1 equiv of imidazole; however, excesses of imidazole led to the formation of a reddish brown tetrameric $\{Fe(NO)_2\}^9$ species, complex **9**. This product, presumed to require adventitious oxygen for oxidation, could be obtained in greater yield in the presence of excess imidazole. Its structure is described below.

The NHC products **1**−**4** were isolated as air sensitive, thermally stable, crystalline solids and subjected to X-ray diffraction analysis, vide infra. Exposure of the $\{Fe(NO)_2\}^{10}$ NHC complexes **1**−**4** to air either as solids or in solution led to eventual degradation under ambient conditions. The air

Scheme 1. Reactions of NHC and Imidazole with $\{Fe(NO)_2\}^{10}$ Precursor

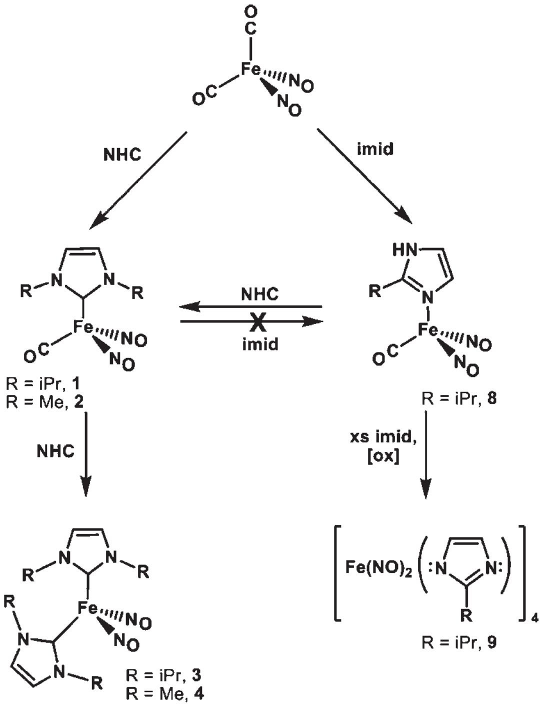

Scheme 2. Synthetic Routes to Oxidized bis-NHC DNICs

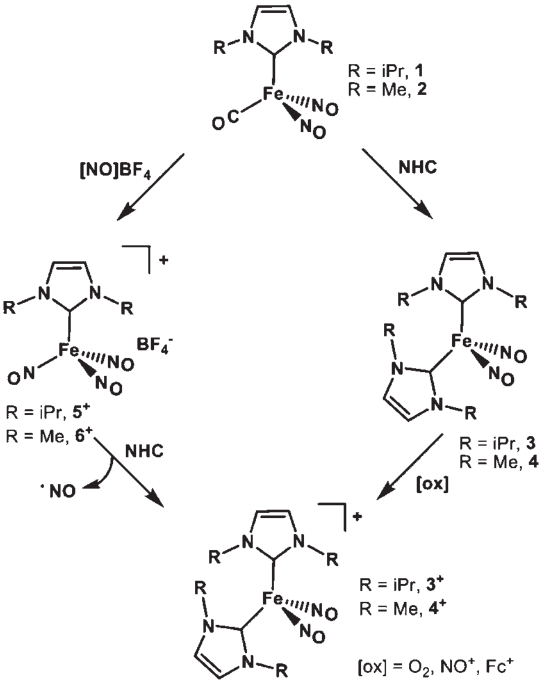

Scheme 3. Comparison of NHC and Imidazole Reacting with $\{Fe(NO)_2\}^9$ Precursor

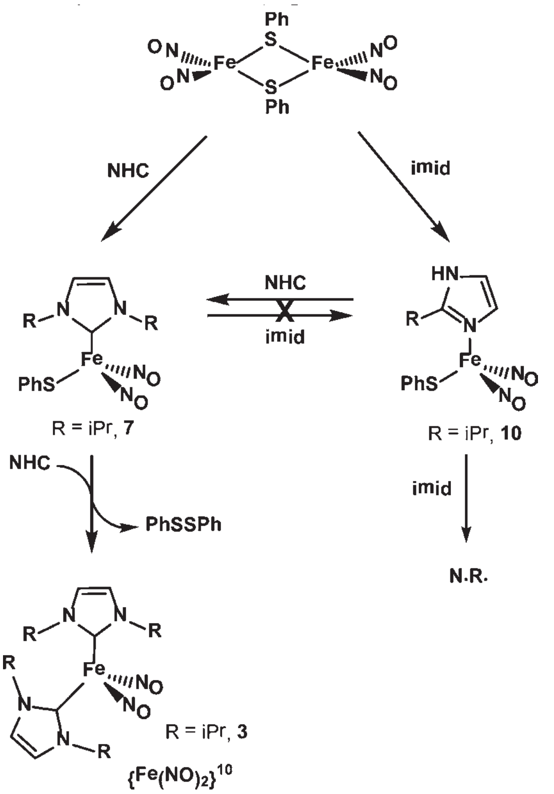

sensitivity in solution was found to be dependent on the NHC substituent, requiring ca. 24 h for degradation of the NHC-*i*Pr DNICs **1** and **3**; within 1 h, the NHC-Me complexes **2** and **4** are oxidized and degraded.

Nevertheless, intermediates in the oxidation process, especially of complexes **3** and **4**, can be observed. Reaction of complexes **3** and **4** with O_2 or NO^+ as oxidant leads to a color change from brown to yellow-brown, with ν(NO) band shifts to higher wavenumbers consistent with the formation of the **3**$^+$ and **4**$^+$ $\{Fe(NO)_2\}^9$ products (Scheme 2). In contrast, addition of NO^+ to complexes **1** and **2** resulted in CO/NO^+ ligand exchange and formation of the green trinitrosyl complexes **5**$^+$ and **6**$^+$, respectively. Treatment of TNICs **5**$^+$ and **6**$^+$ with the appropriate NHC, proceeding with release of NO radicals (identified by capture of NO in a separate solution containing a NO-trapping reagent, that is, a double tube arrangement as described in ref 20), resulted in the formation of complexes **3**$^+$ and **4**$^+$, respectively, with the same color and ν(NO) bands as observed with direct oxidation of complexes **3** and **4**. This latter approach to **5**$^+$ and **6**$^+$ to the DNICs **3**$^+$ and **4**$^+$ appears to give cleaner compounds. Because of instability, as evidenced by the bleaching of color and loss of ν(NO) IR bands, the cationic complexes **3**$^+$ and **4**$^+$ could not be isolated as pure and crystalline materials; however, mass spectral results are consistent with the formulations given.

A common precursor to neutral $\{Fe(NO)_2\}^9$ DNICs is the Roussin's Red "ester", RRE $(\mu\text{-SPh})_2[Fe(NO)_2]_2$ (Scheme 3).[38] Cleavage of this dimeric complex by NHCs or imidazoles leads to analogous DNICs containing one NHC or imidazole and one SPh^- (complexes **7** and **10**). Complete conversion of the RRE dimer required excess (>14 equiv) imidazole, whereas only 2 equiv of NHC was needed for complete conversion of the dimer to (NHC-*i*Pr)(PhS)$Fe(NO)_2$ (**7**), which was isolated and structurally characterized by X-ray diffraction. Subsequent reaction of complex **7**, with additional NHC-*i*Pr, resulted in bimolecular reductive elimination of PhSSPh, with formation of the reduced $\{Fe(NO)_2\}^{10}$ complex **3**. The imidazole complex **10** is unreactive with excess imidazole.

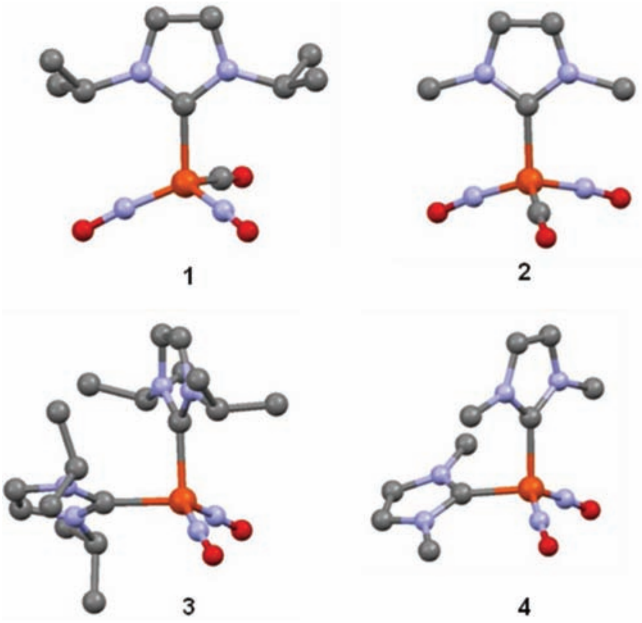

Figure 3. As derived from X-ray diffraction analysis, ball-and-stick structures of the $\{Fe(NO)_2\}^{10}$ complexes: **1** = (NHC-*i*Pr)(CO)Fe(NO)$_2$, **2** = (NHC-Me)(CO)Fe(NO)$_2$, **3** = (NHC-*i*Pr)$_2$Fe(NO)$_2$, and **4** = (NHC-Me)$_2$Fe(NO)$_2$. Hydrogen atoms have been removed for clarity. Thermal ellipsoid plots are given in the Supporting Information. Selected metric data are in Table 1.

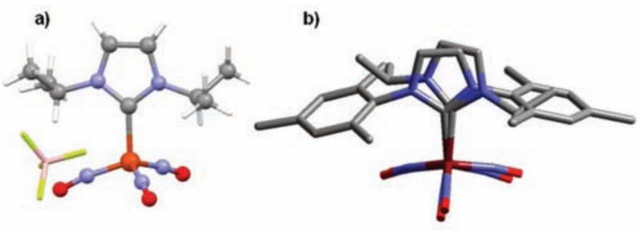

Figure 4. (a) Ball-and-stick structure of the trinitrosyl (NHC-*i*Pr) Fe(NO)$_3^+$ BF$_4^-$ salt, complex **5**$^+$. (b) Overlay of the (NHC-Mes)Fe(NO)$_3^{+20}$ with TNIC **5**$^+$.

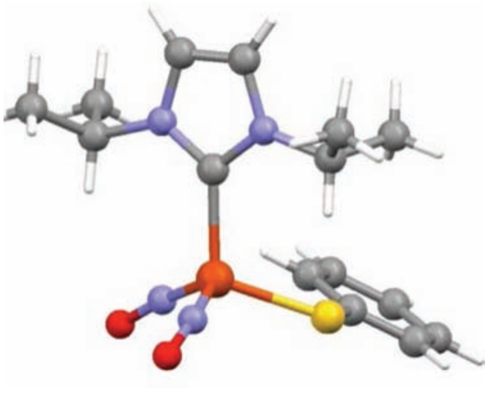

Figure 5. Solid-state molecular structure of (NHC-*i*Pr)(PhS)Fe(NO)$_2$, complex **7**, in ball-and-stick form. Thermal ellipsoid plots are given in the Supporting Information.

Molecular Structures. The molecular structures of complexes **1**, **2**, **3**, **4**, **5**$^+$, and **7** were determined by X-ray diffraction analysis and are represented in ball-and-stick form in Figures 3−5. Full structure reports are available in the Supporting Information, as are thermal ellipsoid plots. Selected metric data for these complexes are presented in Table 1. The monomeric DNIC complexes are pseudotetrahedral, with average $C_{NHC}-Fe-N_{NO}$ bond angles in the range of 107−109°. The $N_{NO}-Fe-N_{NO}$ angles in complexes **3** and **4** are 119° and 122°, and the $C_{NHC}-Fe-C_{NHC}$ bond angles of complexes **3** and **4** are 90° and 96°, respectively. This distortion from standard tetrahedral angles is similar to that of other neutral L$_2$Fe(NO)$_2$ complexes of $\{Fe(NO)_2\}^{10}$ composition, including Wang et al.'s (Imid-Me)$_2$Fe(NO)$_2$ complex, in which the $\angle N_{imid}-Fe-N_{imid}$ is 91.2°.[14] The Fe−N−O bond angles are substantially linear for the $\{Fe(NO)_2\}^{10}$ complexes with an average of 174°. The bis-imidazole complex (Imid-Me)$_2$Fe(NO)$_2$ has somewhat bent Fe−N−O angles of 168°. Likewise for complex **7**, Figure 5, a $\{Fe(NO)_2\}^9$ complex, the $\angle$Fe−N−O averages to 167°, with the N−O ligands oriented inward toward each other, as was observed for the $\{Fe(NO)_2\}^9$ complex, (NHC-Mes)(SPh)Fe(NO)$_2$.[20] All in all, the L$_2$Fe(NO)$_2$ complex structures are similar to each other and to structures of LXFe(NO)$_2$ complexes, even when the spectator ligands are within bidentate frameworks.[18,19]

The $\{Fe(NO)_3\}^{10}$ complex **5**$^+$ is an uncommon, trinitrosyliron complex, TNIC, stabilized by the NHC-*i*Pr (Figure 4a). The (NHC-Mes)Fe(NO)$_3^+$ complex is a precise analogue of **5**$^+$.[20] An overlay of the molecular structures of TNIC **5**$^+$ and (NHC-Mes)-Fe(NO)$_3^+$ is given in Figure 4b. The average $\angle N_{NO}-Fe-N_{NO}$ of 112.3° of the TNICs reflects a narrow range of angles; that is, the bulk of the NHC does not influence one NO position over another. The steric bulk of the pendant N-substituents on the NHC rings undoubtedly contributes to the stability of these TNICs. In support of this conclusion, the (NHC-Me)Fe(NO)$_3^+$ cation, complex **6**$^+$, did not lend itself to crystallization because of instability in solution. This is similar to other reported TNICs, such as those derived from phosphines.[20,39]

The molecular structure of complex **9** was also determined by X-ray crystallographic analysis and is shown in Figure 6. This tetrameric structure is similar to the unsubstituted imidazole-containing tetramer ([(Im-H)Fe(NO)$_2$]$_4$) reported by Wang and Li et al.[40] In both structures, the irons are the corners of a square plane (average deviation from the best plane is 0.0175 Å for complex **9** and 0.0094 Å for [(Im-H)Fe(NO)$_2$]$_4$) with deprotonated imidazole units as bridges along the edges and nitrosyl ligands capping the corners. Select metric parameters of both complexes are given in Table 2. A major difference in the two is the orientation of the methenyl or ethenyl groups with respect to the Fe$_4$ plane. In complex **9**, alternating up/down orientations minimize the steric interaction of the *i*-Pr groups. In the simpler unsubstituted imidazole, the methylene units are all positioned on one side while the opposite ethenyl units produce a bowl-like arrangement in which an acetone molecule resides as a solvent of crystallization. The imidazole planes intersect the Fe$_4$ plane at an average 71° for complex **9** and 53° for [(Im-H)Fe(NO)$_2$]$_4$. The average Fe-to-Fe distances are 6.24 Å in complex **9** (5.97 Å in the unsubstituted imidazole analogue). The overall dimensions of the cyclic tetramer of 8.76 Å × 8.90 Å, defined as the distances between opposite irons in the metallocycle, (Fe1···Fe3 × Fe2···Fe4), are larger than those of [(Im-H)Fe(NO)$_2$]$_4$ (8.18 Å × 8.70 Å), likely to accommodate the additional steric bulk of the isopropyl groups on the 2-position of the imidazole ring.

Table 1. Selected Bond Distances (Å) and Angles (°) for Molecular Structures **1**−**5**$^+$ and **7**

	1	2	3	4	5$^+$	7
			bond distances (Å)			
Fe−C$_{NHC}$	2.005(2)	2.025(6)	2.015(3)	1.973(6)	2.004(5)	2.062(2)
Fe−NO avg	1.675(2)	1.727(6)	1.642(3)	1.659(6)	1.692(5)	1.668(3)
Fe−CO	1.784(2)	1.729(6)				
Fe−S						2.256(11)
N−O avg	1.181(2)	1.176(7)	1.204(3)	1.202(6)	1.151(6)	1.172(3)
			bond angles (°)			
N$_{NO}$−Fe−N$_{NO}$	119.07(10)	111.3(2)	119.48(19)	121.9(3)	112.3(3)[a]	113.80(13)
Fe−N−O avg	175.8(2)	173.3(5)	173.8(2)	174.0(5)	172.8(4)	166.8(3)
C$_{NHC}$−Fe−N$_{NO}$ avg	107.9(8)	107.6(3)	109.39(11)	109.7(2)	106.5(2)	108.93(13)
C$_{NHC}$−Fe−C$_{NHC}$			89.72(17)	96.4(2)		
C$_{NHC}$−Fe−S						110.79(9)
C$_{NHC}$−Fe−CO	99.04(9)	103.6(2)				

[a] Average of angles.

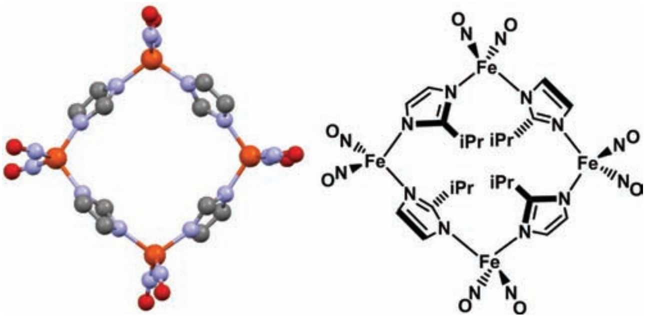

Figure 6. Left: from X-ray diffraction analysis, a ball-and-stick rendering of the molecular structure of complex **9** (isopropyl groups have been removed for clarity). Right: the analogous ChemDraw representation of **9**.

Table 2. Selected Bond Distances (Å) and Angles (°) in Complex **9** and Imidazole Analogue[40]

	9	[(Im-H)Fe(NO)$_2$]$_4$
avg	bond distances (Å)	
Fe−N$_{Imid}$	2.036(11)	2.005(5)
N−O	1.194(13)	1.166(6)
Fe−N$_{NO}$	1.712(13)	1.694(5)
Fe···Fe (adj)	6.241	5.971
Fe···Fe (cross)	8.827	8.440
	bond angles (°)	
N$_{Imid}$−Fe−N$_{Imid}$	110.72(5)	109.24(17)
N$_{NO}$−Fe−N$_{NO}$	110.39(5)	114.8(2)
Fe−N−O	164.02(11)	166.8(6)

Infrared Spectral Data. Table 3 lists the diatomic ligand stretching frequencies for the DNIC complexes of this study as well as other complexes selected for appropriate comparisons. Typically, DNICs of the $\{Fe(NO)_2\}^{10}$ configuration have ν(NO) stretching frequencies in the 1620−1740 cm^{-1} range, whereas those of the oxidized $\{Fe(NO)_2\}^9$ form are shifted positively into the 1700−1800 cm^{-1} regime. Cationic $\{Fe(NO)_2\}^9$ derivatives have higher ν(NO) than neutral analogues, demonstrated in this study by the differences in values for complex **3**$^+$ and complex **7**. Notably, the difference between ν(NO) values of neutral complex **3**, of the $\{Fe(NO)_2\}^{10}$ configuration, and cationic complex **3**$^+$, is over 100 cm^{-1}, whereas the difference between the neutral $\{Fe(NO)_2\}^9$ complex, (NHC-*i*Pr)(PhS)Fe(NO)$_2$, and the anionic $\{Fe(NO)_2\}^9$ complex, $(PhS)_2Fe(NO)_2^-$, is only 20 cm^{-1}.[10] This phenomenon is consistent with the differences of ν(NO) stretching frequencies between (sparteine)Fe(NO)$_2^{0/+}$ and (RS)$_2$-Fe(NO)$_2^-$ versus (Imid)(SR)Fe(NO)$_2$ (R = Ph-*o*-NH-CO-Ph).[10,41] As the structural differences in Fe−N−O distances and angles is minimal, the source of these major discrepancies awaits computational delineation.

Where comparisons of NHC and imidazole complexes are appropriate, both ν(NO) and ν(CO) values suggest that the former is the (slightly) better donor. The better donating ability of NHC ligands as reported by ν(CO) values in NHC/CO transition-metal complexes has been established. Thus, in the case of the tetrahedral DNIC complexes, both steric properties and electron-donor properties of the NHC ligands should make them suitable mimics of imidazole ligands.

Table 4 lists ν(NO) infrared results for the cationic $\{Fe(NO)_3\}^{10}$ complexes with NHC and phosphine ligands. The higher stretching frequencies of these complexes speak to the replacement of CO by the isoelectronic NO$^+$ ligand in, for example, complexes **1** and **2**, yielding a typical pattern of pseudo C_{3v} symmetry.

Electron Paramagnetic Resonance Spectral Data and Magnetic Susceptibility of Complex 9. The EPR spectra for the following paramagnetic $\{Fe(NO)_2\}^9$ complexes prepared in this study were recorded at 10 and 295 K in THF solution: **3**$^+$, **4**$^+$, **7**, **9**, and (Imid-*i*Pr$^-$)$_2$Fe(NO)$_2^-$ (vide infra). At room temperature, complexes **3**$^+$, **4**$^+$, and **7** show isotropic signals at g = 2.028, 2.057, and 2.026, respectively. These are listed and compared with analogous complexes in Table 5. Example spectra are displayed in Figure 7. The EPR spectra for the anionic, bis-imidazolate DNIC complexes show rhombicity with g values, for example, of 2.038, 2.027, and 2.008 for (Imid-*i*Pr$^-$)$_2$Fe(NO)$_2^-$.

According to the report of Wang and Li et al., the EPR spectrum of a frozen THF solution of tetrameric [(Im-H)Fe-(NO)$_2$]$_4$ (based on the unsubstituted imidazolate) shows a nine-line spectrum with N-14 hyperfine coupling superimposed on a

Table 3. ν(NO) Values for Selected DNICs Containing S, N, and C Donors[e]

		$LL'Fe(NO)_2$		ν(CO) cm^{-1} (THF)	ν(NO) cm^{-1} (THF)	
	complex	L	L′		sym, asym	ref
neutral $\{Fe(NO)_2\}^{10}$		CO	CO	2089(m), 2038(s)	1807(m), 1762(s)	27
	1	CO	NHC-*i*Pr	1988(m)	1738(m), 1696(s)	[a]
	2	CO	NHC-Me	1986(m)	1740(m), 1697(s)	[a]
	8	CO	Imid-*i*Pr	1992(m)	1744(m), 1698(s)	[a]
	3	NHC-*i*Pr	NHC-*i*Pr		1664(m), 1619(s)	[a]
	4	NHC-Me	NHC-Me		1667(m), 1624(s)	[a]
		Imid-Me	Imid-Me		1673(m), 1616(s)	14
		sparteine[b]			1679(m), 1622(s)	10
anionic $\{Fe(NO)_2\}^{10}$		Ar-nacnac[c]			1627(m), 1567(s)[d]	42
cationic $\{Fe(NO)_2\}^{9}$	$\mathbf{3}^+$	NHC-*i*Pr	NHC-*i*Pr		1791(m), 1723(s)	[a]
	$\mathbf{4}^+$	NHC-Me	NHC-Me		1789(m), 1733(s)	[a]
		sparteine			1808(m), 1739(s)	10
neutral $\{Fe(NO)_2\}^{9}$	**7**	NHC-*i*Pr	SPh		1757(m), 1712(s)	[a]
		NHC-Mes	SPh		1763(m), 1715(s)	20
	10	Imid-*i*Pr	SPh		1767(m), 1715(s)	[a]
	9	Imid-*i*Pr$^-$	Imid-*i*Pr		1794(m), 1726(s)	[a]
		Ar-nacnac			1761(m), 1709(s)[d]	42
anionic $\{Fe(NO)_2\}^{9}$		Imid-*i*Pr$^-$	Imid-*i*Pr$^-$		1765(m), 1699(s)	[a]
		Imid$^-$	Imid$^-$		1774(m), 1712(s)	15
		SPh	SPh		1737(m), 1693(s)	10

[a] This work. [b] Sparteine = (6*R*,8*S*,10*R*,12*S*)-7,15-diazatetracyclo[7.7.1.0^{2,7}.0^{10,15}]heptadecane. [c] Ar-nacnac = [(2,6-diisopropylphenyl)NC(Me)]$_2$CH. [d] Benzene-d_6 solution measurements. [e] THF solution measurements except where noted.

Table 4. ν(NO) Values for TNICs Containing P, N, and C Donors[e]

		L	ν(NO) cm^{-1}	ref
cationic $\{Fe(NO)_3\}^{10}$	$\mathbf{5}^+$	NHC-*i*Pr	1915(m), 1826(sh), 1810(s)	[a]
	$\mathbf{6}^+$	NHC-Me	1915(m), 1825(sh), 1814(s)	[a]
		NHC-Mes	1932(s), 1831(s), 1804(vs)[b]	20
		P(*p*-Tolyl)$_3$	1917(s), 1838(vs), 1813(vs)[c]	20
		$P(CH_2OH)_3$	1927(w), 1833(vs)[d]	39
		EtCN	1939(w), 1836(s)	43

[a] This work. [b] In THF. [c] Solid, ATR-FTIR. [d] In nitromethane. [e] CH_2Cl_2 solution measurements.

Table 5. EPR-Derived *g* Values of Selected DNIC in THF Solution at Low Temperatures As Indicated

complex	*g* value	temp (K)	ref
$\mathbf{3}^+$	2.028	10	[a]
$\mathbf{4}^+$	2.057	10	[a]
$(Imid\text{-}Me)_2Fe(NO)_2^+$	2.015	240	14
7	2.026	10	[a]
(NHC-Mes)(SPh)Fe(NO)$_2$	2.049, 2.029, 2.013	77	20
(Ar-nacnac)Fe(NO)$_2$	2.09, 2.06, 2.05	77	42
(Imid-*i*Pr$^-$)$_2$Fe(NO)$_2^-$	2.038, 2.027, 2.008	10	[a]
(Imid$^-$)$_2$Fe(NO)$_2^-$	2.040, 2.022, 2.013	77	15
9	2.055, 2.029, 2.012	10	[a]
$[(Im\text{-}H)Fe(NO)_2]_4$	2.031	170	40
(Imid)(SPh-*o*-NH−CO-Ph)Fe(NO)$_2$	2.031	298	41

[a] This work.

rhombic signal.[40] Preliminary EPR spectral data taken on a solution of the analogous complex **9** show a broad rhombic signal with *g* values of 2.055, 2.029, and 2.012 at 10 K that appears to be an unresolved rhombic envelope of the 9-line spectrum reported by Wang and Li et al.[40] As of this report, further resolution of the spectrum of **9** into hyperfine features has not been achieved. At 295 K, the signal becomes isotropic with a *g* value of 2.033. Interestingly, the imidazolate-cleaved tetramer of Wang and Li et al., the (Imid$^-$)$_2$Fe(NO)$_2^-$ anion, also shows hyperfine coupling.[15] This feature is not observed for the bis-Imid-*i*Pr anion described above.

It is well known that spin−spin coupling between $\{Fe(NO)_2\}^9$ units occurs in clusters, such as Roussin's Red ester (Fe−Fe separation = 2.5−2.6 Å), resulting in EPR silent complexes. In a dimer designed to have an Fe−Fe separation of ca. 4 Å, an EPR signal is observed.[6] Hence, as the separation between $\{Fe(NO)_2\}^9$ units in the imidazolate tetramers under discussion here is ca. 6 Å, spin−spin coupling is not expected. This is confirmed for complex **9** by the room-temperature (Gouy balance) magnetic susceptibility measurement yielding an effective magnetic moment per Fe atom, μ_{eff}, of 1.75 μ_B (theoretical μ_{SO} value for one unpaired electron per Fe is 1.73 μ_B).

Rather than attribute the hyperfine observed in the EPR spectrum of $[(Im\text{-}H)Fe(NO)_2]_4$ to N-14 coupling within the intact tetramer, Wang and Li et al. have suggested that the simpler complex dissociates in THF solvent, producing an [(Imid$^-$)(THF)Fe(NO)$_2$] monomeric DNIC with N-14 coupling from nitrogens of two nitrosyls and one imidazolate ligand, accounting for the 9-line spectrum.[40] In support of this conclusion, Tsai and

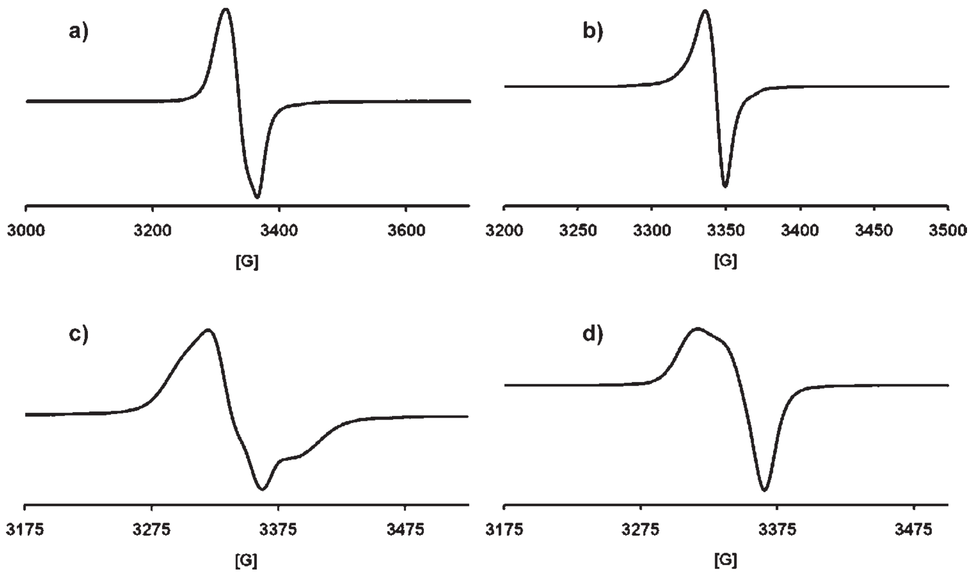

Figure 7. X-band EPR spectra taken at 10 K in a THF solution of (a) complex 3^+ with a frequency at 9.468 GHz, (b) complex **7** with a frequency at 9.482 GHz, (c) complex **9** with a frequency at 9.468 GHz, and (d) complex (Imid-*i*Pr$^-$)$_2$Fe(NO)$_2$$^-$ as a Na-18-crown-6-ether salt with a frequency at 9.473 GHz.

Table 6. Electrochemical Potentials of Selected DNICs and TNICs[a]

	E_{pc} (V)	$E_{1/2}$ (V)	ref
1	0.14		[b]
2	0.12		[b]
(CO)(NHC-Mes)Fe(NO)$_2$	−0.34		20
3		−0.76	[b]
4		−0.77	[b]
(bipy)Fe(NO)$_2$		−0.48	44
$\mathbf{5}^+$		0.90[c]	[b]
(NHC-Mes)Fe(NO)$_3$$^+$		−0.29 (−0.395)[c]	20
7		−1.33	[b]
(NHC-Mes)(SPh)Fe(NO)$_2$		−1.48	20
(Ar-nacnac)Fe(NO)$_2$		−1.34	42

[a] In THF solution (0.1 M ^{t}Bu$_4$NBF$_4$). All experiments were recorded using a glassy carbon working electrode and Pt counter electrode and referenced to Cp$_2$Fe/Cp$_2$Fe$^+$ at a scan rate of 100 mV/s. [b] This work. [c] In CH$_2$Cl$_2$ solution.

Liaw et al. report a monomeric $\{Fe(NO)_2\}^9$ complex, (Imid)(SR)Fe(NO)$_2$ (R = Ph-*o*-NH-CO-Ph), with two nitrosyls and one imidazole, which also exhibits a well-resolved 9-line EPR signal centered at $g = 2.031$ with hyperfine coupling constants of 2.4 and 4.1 G at 298 K;[41] these are among the few observations of such hyperfine coupling in paramagnetic DNICs. We note that the ν(NO) IR spectra of complex **9** in THF solution and in the solid state are identical. Hence, at this stage of investigation, there is no compelling evidence for breakup of the tetramer in solution; however, the lack of resolvable features in the EPR spectrum of complex **9** deserves further inquiry.

Cyclic Voltammetry. Cyclic voltammograms of complexes **1**, **2**, **3**, **4**, and **7** were recorded in 2 mM THF solution, and complex $\mathbf{5}^+$ was recorded in 2 mM CH$_2$Cl$_2$ solution with 100 mM [*t*-Bu$_4$N][BF$_4$] as the supporting electrolyte. All potentials were measured relative to a Ag/AgNO$_3$ electrode using a glassy carbon working electrode and are referenced to Cp$_2$Fe/Cp$_2$Fe$^+$. The redox potentials for each complex are given in Table 6, and selected CVs are shown in Figure 8. For complexes **1** and **2**, an irreversible oxidation event occurs at 0.14 and 0.12 V, respectively, whereas for complexes **3** and **4**, a reversible redox couple assigned to the $\{Fe(NO)_2\}^{9/10}$ couple is centered at −0.76 and −0.77 V, respectively (Figure 8b). Compared to the previously reported neutral-$\{Fe(NO)_2\}^{10}$, (bipy)Fe(NO)$_2$ (bipy = 2,2′-bipyridine), which has a reversible redox event at −0.48 V,[44] the neutral, bis-NHC-containing DNICs are oxidized at more negative values, ca. −0.76 V, which is consistent with the stronger electron-donating characteristics of the NHC ligands. Despite the reversibility of the cationic complex $\mathbf{5}^+$ couple at 0.90 V (recorded in CH$_2$Cl$_2$ due to insolubility in THF), the TNIC rapidly decomposed with repeated scans. Note that the reversible reduction of the analogous NHC-Mes TNIC is more negative by a volt ($E_{1/2} = -0.29$ V in THF and −0.39 V in CH$_2$Cl$_2$) than that of $\mathbf{5}^+$.[20] This major discrepancy is not understood.

Complex **7** has a reversible redox event at −1.33 V (measured in THF), and similar to the previously reported (NHC-Mes)(PhS)Fe(NO)$_2$ complex, the reversible process is scan-rate-dependent.[20] It is notable that the (Ar-nacnac)Fe(NO)$_2$$^{0/1-}$ complex couple is at −1.34 V in THF solution,[42] closely matching the reversible $\{Fe(NO)_2\}^{9/10}$ couple of complexes **7** and (NHC-Mes)(PhS)Fe(NO)$_2$, but almost a volt more negative than the couple for (bipy)Fe(NO)$_2$.

Overall, these data affirm that the redox properties of the Fe(NO)$_2$ unit respond to the ligand environment in a manner reflecting the typical donor/acceptor abilities of the spectator ligands.

Reactivity Studies. As noted above, imidazoles cleave the RRE (μ-SPh)$_2$[Fe(NO)$_2$]$_2$ to form the (Imid-R)(SPh)Fe(NO)$_2$ complex. The imidazole ligand can, subsequently, be displaced by addition of NHC-*i*Pr to form complex **7**; addition of imidazole, even in large excesses, does not result in NHC displacement. Likewise, in the $\{Fe(NO)_2\}^{10}$ cases, addition of imidazole to Fe(CO)$_2$(NO)$_2$

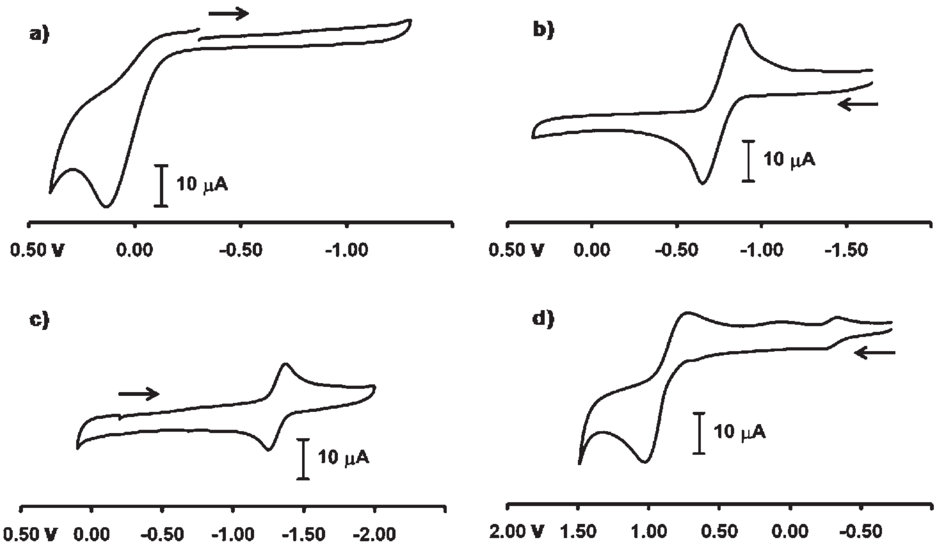

Figure 8. Cyclic voltammograms of complexes (a) **1**, (b) **3**, (c) **7** in 2 mM THF solution, and (d) **5**$^+$ in 2 mM CH_2Cl_2 solution. All are referenced to Cp_2Fe/Cp_2Fe^+.

Scheme 4. Reactivity of Complex 3$^+$ with NaSPh in THF Solvent

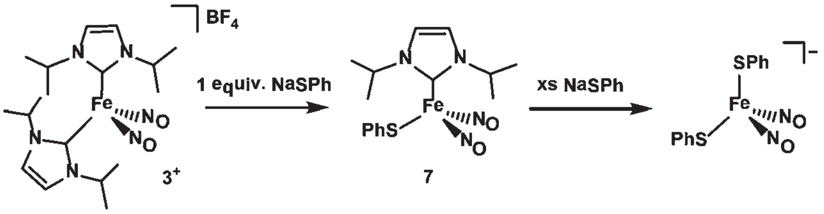

results in the formation of (Imid-R)(CO)Fe(NO)$_2$. Again, the imidazole is readily (within minutes) displaced upon addition of NHC to form complexes **1** and **2**, in an irreversible reaction (Scheme 1). Addition of excess NHC-*i*Pr to complex **7** results in the formation of complex **3** with bimolecular reductive elimination of diphenyl disulfide; however, addition of excess imidazole to (Imid)(SPh)Fe(NO)$_2$ had no effect, as reported in Scheme 3. No reaction occurred on addition of NaSPh to reduced complex **3**; however, 1 equiv of NaSPh displaced NHC-*i*Pr from oxidized complex **3**$^+$ to form complex **7** (Scheme 4). Further addition of an excess of NaSPh to **3** results in the formation of $(SPh)_2Fe(NO)_2^-$. In the neutral $\{Fe(NO)_2\}^9$ complexes, the replacement of imidazole by the stronger donating NHC likely results in a stabilized oxidized iron unit. Nevertheless, anionic thiolates are even better stabilizers of the oxidized $\{Fe(NO)_2\}^9$ unit, as exemplified by the instability of the cationic $(NHC)_2Fe(NO)_2^+$ complexes. The neutral, paramagnetic (NHC)(PhS)Fe(NO)$_2$ are perhaps the most stable of the complexes explored in this study, whereas the neutral, diamagnetic $(NHC)_2Fe(NO)_2$ are the second most stable. Again, the remarkable ability of the N-heterocyclic carbenes to stabilize two redox levels is noted. Interestingly, the PhS$^-$ anions did not appear to extract NO, forming PhSNO, in a decomposition side reaction, in any of the reactions explored.

Imidazole-Containing Analogues. The tetrameric complex **9**, resulting from attempts to prepare monomeric complex **8** (Scheme 1), can be cleaved with deprotonated Imid-*i*Pr to form the anionic $(Imid\text{-}iPr^-)_2Fe(NO)_2^-$ complex, containing the oxidized $\{Fe(NO)_2\}^9$ unit, as demonstrated via IR and EPR spectroscopies. Consistent with the results of Chen et al. working with the unsubstituted $[(Im\text{-}H)Fe(NO)_2]_4$ cluster, complex **9** can also be cleaved by deprotonated phenyl thiolate to form the mononuclear, $(Imid^-)(SPh)Fe(NO)_2^-$ DNIC.[16] The formation of clusters is highly relevant to thiolate-containing DNICs. Vanin et al. have reported that this type of reactivity, under biological conditions using cysteine and glutathione, can be regulated by the pH, where a decrease to pH = 5 results in formation of dinuclear $\{Fe(NO)_2\}^9$ DNICs and an increase to a pH of 9−10 results in the formation of mononuclear $\{Fe(NO)_2\}^9$ DNICs.[45] Additionally, it has been established that, in biological systems in the absence of excess thiol, diamagnetic, spin-coupled dinuclear DNICs are formed rather than the paramagnetic mononuclear DNICs.[46] Thus, from our studies with imidazole-containing DNICs, it is reasonable that similar reactivity modulated by pH and the presence or absence of histidine/imidazole could control formation of polynuclear versus mononuclear DNICs.

NO-Transfer Studies. To probe the ability of the NHC-containing DNICs to release or transfer NO, the DNICs were combined with the NO-trapping reagent Co(TPP) in THF solution. Coupled with an almost immediate color change, an IR band that grew in at 1683 cm^{-1} concomitant with loss of bands from the DNIC, indicated (NO)Co(TPP) formation.[37] This reactivity of oxidized $\{Fe(NO)_2\}_9$ complexes **3**$^+$ and **4**$^+$ was in great contrast to the reduced $\{Fe(NO)_2\}^{10}$ complexes **3** and **4**, which showed no change upon mixing with THF solutions of Co(TPP). This preliminary study suggests that DNICs in the reduced $\{Fe(NO)_2\}^{10}$ oxidation level are inert to NO loss/transfer, whereas DNICs in the oxidized $\{Fe(NO)_2\}^{9}$ oxidation state are sources of NO in the presence of a suitable NO-trapping agent. This conclusion is supported by the work of Chiang et al. and Tonzetich et al.[37,42] Such assenting results encourage future studies to develop a biologically compatible DNIC that can be "turned on" by oxidation to deliver NO to a specific target. Nevertheless, the mechanism of NO transfer is unknown, neither is the fate of the DNIC following loss of NO. From "double-tube" experiments, we have shown that the cationic NHC−TNIC complex stabilized by the bulky NHC-Mes releases NO as free NO radical/gas, which can diffuse into a solution containing a NO-trapping reagent.[20] Such a design to explore NO release from $\mathbf{3}^+$ or $\mathbf{4}^+$ was not successful.

SUMMARY AND COMMENTS

This work demonstrates that N-heterocyclic carbene ligands (NHCs) are suitable as mimics of imidazole and histidine. From the above demonstrated syntheses and reactivity, and chemical precedent, it can be concluded that the $\{Fe(NO)_2\}^{10}$ unit coexists with neutral ligands, such as CO, phosphines, NHCs, and imidazoles. The $\{Fe(NO)_2\}^{9}$ unit is stable in the presence of anionic ligands, such as SR^-, deprotonated imidazoles, or mixed anionic/neutral ligand sets, neutral ligands being NHCs. Additionally, the precursors to $\{Fe(NO)_2\}^{10}$ and $\{Fe(NO)_2\}^{9}$, $Fe(CO)_2(NO)_2$, and $(\mu\text{-RS})_2[Fe(NO)_2]_2$, respectively, are both susceptible to reaction with imidazoles as well as NHCs. In the latter case, trinitrosyl iron complexes may be derived. N-heterocyclic carbene ligands also stabilize neutral $\{Fe(NO)_2\}^{10}$, neutral $\{Fe(NO)_2\}^{9}$, and cationic $\{Fe(NO)_2\}^{9}$ DNICs. The NO-releasing order in these derivatives is as follows:

$$\{Fe(NO)_3\}^{10}\ \text{TNICs} > \{Fe(NO)_2\}^{9}\ \text{DNICs} \gg \{Fe(NO)_2\}^{10}\ \text{DNICs}$$

When deprotonated, the distal nitrogen functionality in the imidazole ligands of $[(Imid)_2Fe(NO)_2]^-$ imidazolates can lead to aggregation through bridging, illustrated here in the new tetrameric complex **9**. Such interesting molecular squares are composed of $\{Fe(NO)_2\}^{9}$ units. Magnetic susceptibility data demonstrate that each Fe within the tetramer can be considered as noncoupled, $S = 1/2$, units at room temperature. Temperature-dependent magnetic properties of **9** and analogues and the effect of sterically encumbered imidazoles on structure and aggregation are currently under investigation.

ASSOCIATED CONTENT

Supporting Information. X-ray crystallographic data (CIF) from the structure determinations, TEPs, and full lists of metric parameters for complexes **1**−**4**, $\mathbf{5}^+$, **7**, and **9** and mass spectral scans for complex **9**. This material is available free of charge via the Internet at http://pubs.acs.org.

AUTHOR INFORMATION

Corresponding Author

*E-mail: marcetta@chem.tamu.edu.

ACKNOWLEDGMENT

We appreciate financial support from the National Science Foundation (CHE-0910679) and the R. A. Welch Foundation (A-0924). We thank Dr. Timothy Hughbanks (TAMU) and Dr. Andrey Prosvirin (TAMU) for their helpful discussions regarding the EPR data. We also thank Jason Denny (TAMU) for assistance with the X-ray studies, and Dr. Yohannes Rezenom for the mass spectrometry results. Kelsey Shogren, an NSF-REU student, the summer of 2010, contributed to the syntheses of complexes 1−4.

REFERENCES

(1) (a) Vithayathil, A. J.; Ternberg, J. L.; Commoner, B. *Nature* **1965**, *207*, 1246–1249. (b) Woolum, J. C.; Commoner, B. *Biochim. Biophys. Acta* **1970**, *201*, 131–140.

(2) Vanin, A. F. *Nitric Oxide* **2009**, *21*, 1–13.

(3) Foster, M. W.; Cowan, J. A. *J. Am. Chem. Soc.* **1999**, *121*, 4093–4100.

(4) Ostrowski, A. D.; Ford, P. C. *Dalton Trans.* **2009**, 10660–10669.

(5) Chen, Y.-J.; Ku, W.-C.; Feng, L.-T.; Tsai, M.-L.; Hsieh, C.-H.; Hsu, W.-H.; Liaw, W.-F.; Hung, C.-H.; Chen, Y.-J. *J. Am. Chem. Soc.* **2008**, *130*, 10929–10938.

(6) Tsai, M.-L.; Hsieh, C.-H.; Liaw, W.-F. *Inorg. Chem.* **2007**, *46*, 5110–5117 and references therein.

(7) Cesareo, E.; Parker, L. J.; Pedersen, J. Z.; Nuccetelli, M.; Mazzetti, A. P.; Pastore, A.; Federici, G.; Caccuri, A. M.; Ricci, G.; Adams, J. J.; Parker, M. W.; Lo Bello, M. *J. Biol. Chem.* **2005**, *280*, 42172–42180.

(8) Chiang, C.-Y.; Miller, M. L.; Reibenspies, J. H.; Darensbourg, M. Y. *J. Am. Chem. Soc.* **2004**, *126*, 10867–10874.

(9) Tsai, F.-T.; Chiou, S.-J.; Tsai, M.-C.; Tsai, M.-L.; Huang, H.-W.; Chiang, M.-H.; Liaw, W.-F. *Inorg. Chem.* **2005**, *44*, 5872–5881.

(10) Hung, M.-C.; Tsai, M.-C.; Lee, G.-H.; Liaw, W.-F. *Inorg. Chem.* **2006**, *45*, 6041–6047.

(11) Chiou, S.-J.; Wang, C.-C.; Chang, C.-M. *J. Organomet. Chem.* **2008**, *693*, 3582–3586.

(12) Lu, T.-T.; Tsou, C.-C.; Huang, H.-W.; Hsu, I.-J.; Chen, J.-M.; Kuo, T.-S.; Wang, Y.; Liaw, W.-F. *Inorg. Chem.* **2008**, *47*, 6040–6050.

(13) Enemark, J. H.; Feltham, R. D. *Coord. Chem. Rev.* **1974**, *13*, 339–406.

(14) Reginato, N.; McCrory, C. T. C.; Pervitsky, D.; Li, L. *J. Am. Chem. Soc.* **1999**, *121*, 10217–10218.

(15) Huang, H.-W.; Tsou, C.-C.; Kuo, T.-S.; Liaw, W.-F. *Inorg. Chem.* **2008**, *47*, 2196–2204.

(16) Chen, C.-H.; Ho, Y.-C.; Lee, G.-H. *J. Organomet. Chem.* **2009**, *694*, 3395–3400.

(17) Tinberg, C. E.; Tonzetich, Z. J.; Wang, H.; Do, L. H.; Yoda, Y.; Cramer, S. P.; Lippard, S. J. *J. Am. Chem. Soc.* **2010**, *132*, 18168–18176.

(18) Harrop, T. C.; Tonzetich, Z. J.; Reisner, E.; Lippard, S. J. *J. Am. Chem. Soc.* **2008**, *130*, 15602–15610.

(19) Li, L. *Comments Inorg. Chem.* **2002**, *23*, 335–353.

(20) Hsieh, C.-H.; Darensbourg, M. Y. *J. Am. Chem. Soc.* **2010**, *132*, 14118–14125.

(21) Cornils, B.; Herrmann, W. A. *Aqueous-Phase Organometallic Catalysis*, 2nd ed.; Wiley-VCH: Weinheim, Germany, 2004.

(22) de Frémont, P.; Marion, N.; Nolan, S. P. *Coord. Chem. Rev.* **2009**, *253*, 862–892.

(23) Jenkins, R. M.; Singleton, M. L.; Leamer, L. A.; Reibenspies, J. H.; Darensbourg, M. Y. *Inorg. Chem.* **2010**, *49*, 5503–5514.

(24) Sini, G.; Eisenstein, O.; Crabtree, R. H. *Inorg. Chem.* **2002**, *41*, 602–604.

(25) Schaub, T.; Backes, M.; Radius, U. *Organometallics* **2006**, *25*, 4196–4206.

(26) Hannig, F.; Kehr, G.; Fröhlich, R.; Erker, G. *J. Organomet. Chem.* **2005**, *690*, 5959–5972.

(27) McBride, D. W.; Stafford, S. L.; Stone, F. G. A. *Inorg. Chem.* **1962**, *1*, 386–388.

(28) Connelly, N. G.; Gardner, C. *J. Chem. Soc., Dalton Trans.* **1976**, 1525–1527.

(29) *WINEPR Simfonia*, version 1.25; Bruker Analytische Messtechnik GmbH: Berlin, 1996.

(30) *SMART: Program for Data Collection on Area Detectors*, version 5.632; Bruker AXS Inc.: Madison, WI, 2005.

(31) *APEX2*, version 2009.7—0; Bruker AXS Inc.: Madison, WI, 2007.

(32) *SAINTPLUS: Program for Reduction of Area Detector Data*, version 6.63; Bruker AXS Inc.: Madison, WI, 2007.

(33) Sheldrick, G. M. *SADABS: Program for Absorption Correction of Area Detector Frames*; Bruker AXS Inc.: Madison, WI, 2001.

(34) Sheldrick, G. M. *SHELXS-97: Program for Crystal Structure Solution*; Universität Göttingen: Göttingen, Germany, 1997.

(35) Sheldrick, G. M. *SHELXL-97: Program for Crystal Structure Refinement*; Universität Göttingen: Göttingen, Germany, 1997.

(36) Macrae, C. F.; Edgington, P. R.; McCabe, P.; Pidcock, E.; Shields, G. P.; Taylor, R.; Towler, M.; van de Streek, J. *J. Appl. Crytsallogr.* **2006**, *39*, 453–457.

(37) Chiang, C.-Y.; Darensbourg, M. Y. *J. Biol. Inorg. Chem.* **2006**, *11*, 359–370.

(38) Rauchfuss, T. B.; Weatherill, T. D. *Inorg. Chem.* **1982**, *21*, 827–830.

(39) Dillinger, S. A. T.; Schmalle, H. W.; Fox, T.; Berke, H. *Dalton Trans.* **2007**, 3562–3571.

(40) Wang, X.; Sundberg, E. B.; Li, L.; Kantardjieff, K. A.; Herron, S. R.; Lim, M.; Ford, P. C. *Chem. Commun.* **2005**, 477–479.

(41) Tsai, M.-L.; Liaw, W.-F. *Inorg. Chem.* **2006**, *45*, 6583–6585.

(42) Tonzetich, Z. J.; Héroguel, F.; Do, L. H.; Lippard, S. J. *Inorg. Chem.* **2011**, *50*, 1570–1579.

(43) Hayton, T. W.; McNeil, W. S.; Patrick, B. O.; Legzdins, P. *J. Am. Chem. Soc.* **2003**, *125*, 12935–12944.

(44) Wang, R.; Wang, X.; Sundberg, E. B.; Nguyen, P.; Grant, G. P. G.; Sheth, C.; Zhao, Q.; Herron, S.; Kantardjieff, K. A.; Li, L. *Inorg. Chem.* **2009**, *48*, 9779–9785.

(45) Vanin, A. F.; Poltorakov, A. P.; Mikoyan, V. D.; Kubrina, L. N.; Burbaev, D. S. *Nitric Oxide* **2010**, *23*, 136–149.

(46) McDonald, C. C.; Phillips, W. D.; Mower, H. F. *J. Am. Chem. Soc.* **1965**, *87*, 3319–3326.